CROATICA CHEMICA ACTA CCACAA **72** (2–3) 575–591 (1999)

ISSN-0011-1643
CCA-2599 *Original Scientific Paper*

X-ray Structure of Gelatinase A Catalytic Domain Complexed with a Hydroxamate Inhibitor*

Venugopal Dhanaraj,[a,#] *Mark G. Williams,*[a,#] *Qi-Zhuang Ye,*[b,§] *Franck Molina,*[a] *Linda L. Johnson,*[b] *Daniel F. Ortwine,*[b] *Alexander Pavlovsky,*[b] *J. Ron Rubin,*[b] *Richard W. Skeean,*[b] *Andy D. White,*[b] *Christine Humblet,*[b] *Donald J. Hupe,*[b] *and Tom L. Blundell* [a,**]

[a] *Department of Biochemistry, University of Cambridge, Tennis Court Road, Cambridge, CB2 1QW, UK*

[b] *Departments of Biochemistry and Chemistry, Parke-Davis Pharmaceutical Research, Division of Warner-Lambert Company, 2800 Plymouth Road, Ann Arbor, Michigan 48105, USA*

Received January 25, 1999; servised April 12, 1999; accepted April 14, 1999

Gelatinase A is a key enzyme in the family of matrix metalloproteinases (matrixins) that are involved in the degradation of the extracellular matrix. As this process is an integral part of tumour cell metastasis and angiogenesis, gelatinase is an important target for therapeutic intervention. The X-ray crystal structure of the gelatinase A catalytic domain (GaCD) complexed with batimastat (BB94), a hydroxamate inhibitor, shows an active site with a large S1' specificity pocket. The structure is similar to previously solved structures of stromelysin catalytic domain (SCD) but with differences in VR1 and VR2, two surface-exposed loops on either side of the entrance to the active site. Comparison of GaCD with other members of the matrix metalloproteinase (MMP) family highlights

---

* Dedicated to Professor Boris Kamenar on the occasion of his 70th birthday.

[#] Joint first author.

[§] Current address: Shanghai Institute of Materia Medica, Chinese Academy of Sciences, Shanghai, China 200031.

** Author to whom correspondence should be addressed.

the conservation of key secondary structural elements and the significant differences in the specificity pockets, knowledge of which should enhance our ability to design specific inhibitors for this important anticancer target.

Key words: inhibitor, matrixin, matrix metalloproteinase-3 (MMP-3), stromelysin-1, MMP-2, gelatinase A, metzincin.

INTRODUCTION

Gelatinase is a matrix metalloproteinase that degrades the major protein components of the extracellular matrix in connective tissues, such as type IV collagen.[1] As degradation of the extracellular matrix is an essential step in tumour cell metastasis and angiogenesis, intensive efforts have been devoted to the discovery of matrix metalloproteinase inhibitors for therapeutic use in the treatment of cancer. Batimastat (BB94) represents a class of inhibitors that were developed by modifying the peptide sequence at the cleavage site of substrates and introducing a hydroxamic acid group as the ligand for the catalytic zinc.[2] Such peptide hydroxamates are, in general, potent, broad-spectrum matrix metalloproteinase inhibitors. Batimastat has been shown to inhibit the metastatic spread of tumour cells[3,4] and has been tested clinically for the treatment of malignant effusions associated with thoracic and peritoneal neoplasms.[5]

Matrix metalloproteinases are homologous zinc endopeptidases belonging to the »metzincin« superfamily.[6] They share a zinc-binding HExxHxxGxxH-consensus motif and a strictly conserved methionine-containing 1,4-turn (Met-turn) adjacent to the catalytic zinc ion. Matrix metalloproteinase have three discrete domains, a propeptide which is cleaved during activation, a zinc-binding catalytic domain, and a carboxy-terminal hœmopexin-like domain (not present in matrilysin) involved in substrate recognition. Studies of the catalytic and hœmopexin-like domains of recombinant matrix metalloproteinases[7–11] show that the catalytic domains show similar activity, specificity and sensitivity against synthetic substrates as the parent enzymes, and so are appropriate models for the structure-based design of inhibitors of the full-length proteins.

The three-dimensional structures of several matrix metalloproteinases have now been published. X-ray crystallographic and NMR studies have produced structures of the catalytic domains of fibroblast collagenase,[12–15] neutrophil collagenase,[16–21] matrilysin,[22] stromelysin-1[23–29] and the C-truncated proenzyme of stromelysin-1.[24] Crystal structures of complexes of stromelysin-1 and membrane type 1 matrix metalloproteinase (MMP-14) and naturally occurring tissue inhibitors of metalloproteinases-1 and -2, respec-

tively, have also been disclosed recently.[28,30] Attempts at solving the crystal structures of matrix metalloproteinases containing additional domains have met only limited success. To date, only the full-length structure of porcine collagenase containing the C-terminal domain has been reported.[31]

A unique 19 kDa insert made up of three tandem repeats of a fibronectin type II unit (the »fibronectin insert«) occurs within the catalytic domain of both gelatinase A and gelatinase B. On the basis of homology, we re-engineered gelatinase A at the gene level by deleting this insert and reconnecting the two fragments of the catalytic domain to form a shorter gelatinase A catalytic domain (GaCD).[32] The reconstructed GaCD is very similar to the catalytic domains of stromelysins and collagenases, and has activities similar to that of full-length gelatinase A against synthetic substrates and the natural protein substrate gelatin.[33]

We now report the first X-ray crystal structure of the human gelatinase A catalytic domain protein complexed with the inhibitor batimastat (BB94). The structure confirms some conclusions based on previously generated homology models,[34] but further provides an accurate structural basis for the design of the next generation of inhibitors with improved selectivity and bioavailability. The detailed insights into the interaction of BB94 with gelatinase A, and comparisons with other matrix metalloproteinase crystal structures,[35] can be used to rationalize observed differences in affinity among known inhibitors.

EXPERIMENTAL

Expression, Crystallisation and X-ray Data Collection

The expression and purification of gelatinase A catalytic domain has been described previously.[33] The protein GaCD used in the structural determination is modified slightly from that originally described by changing residues 105–110 (187–191 stromelysin numbering, the last glycine being referred to as 190A in GaCD) from GFCPDQ to SLGKGV, thus eliminating the cysteine in the sequence. The two constructs GaCD and GCD showed similar enzymatic activity.

Crystals suitable for X-ray analysis were grown by the hanging-drop vapour diffusion method with a ≈15 mg/ml protein solution in 50 mM Tris/HCl in the presence of the inhibitor (which was allowed to equilibrate in the concentrated protein solution for several days), 10 μM $ZnCl_2$, 10 mM $CaCl_2$, and PEG8K. Diffraction data were collected on a MARResearch image plate detector at the Synchrotron Radiation Source, Daresbury, UK. The program DENZO[36] was used to establish the reference orientation of the crystal, to reduce the image plate data, and to refine cell and data collection parameters. Further merging, scaling, correction, and processing of the data were carried out using the program SCALEPACK.[36] A summary of the crystal and X-ray diffraction data is presented in Table I.

TABLE I

Crystallographic data and refinement statistics

Space group	$P4_122$
Unit cell	$a = b = 84.83$ Å; $c = 57.90$ Å; $\alpha = \beta = \gamma = 90°$
Number of molecules per asymmetric unit	1
Wavelength / Å	0.88
Maximum resolution / Å	2.8
Unique reflections	5551
Completeness / %	99.5
R_{merge}[a]	0.130
R_{free}	0.244
R_{cryst}[b]	0.205
RMS bonds[c]	0.008
RMS angles[c]	1.452

[a]$R_{merge} = \Sigma|I - \langle I\rangle|/\Sigma I$, where I is the intensity of an individual measurement, and $\langle I\rangle$ is the mean intensity of this reflection. [b]$R_{cryst} = \Sigma||F_o| - |F_c||/\Sigma|F_o|$, where $|F_o|$ and $|F_c|$ are the observed and calculated structure factor amplitudes, respectively. [c]RMS deviations of bond lengths and angles in the refined structure from ideal values.[42]

Structure Analysis

The gelatinase-inhibitor complex was solved by molecular replacement using the AMORE.[37] The catalytic domain of stromelysin (SCD) has a sequence identity of approximately 60% with GaCD and hence the coordinates of SCD complexes previously solved in this laboratory[26,27,38] (minus the inhibitor, metal ions, and water molecules) was used as the initial models. Computation of the rotation function revealed three peaks above the threshold level of 0.5 S, where S is the height of the largest rotation peak. The top solution (which was selected) was twice the height of the second and third solutions. A single molecule in the asymmetric unit was consistent with the expected number of target molecules in the unit cell. The rotation function solution produced just one significant translation function peak for space group $P4_122$. This solution had a correlation coefficient of 0.49 with an R factor of 0.45. After rigid-body refinement using the FITING routine in AMORE, these values improved to 0.59 and 0.42 respectively.

Model Building and Refinement

A sample of 555 out of 5551 unique reflections from the processed data were selected from thin resolution shells using the program DATAMAN,[39] and excluded from the refinement. The agreement between calculated and observed structure fac-

tors for these reflections, R_{free},[40] was used to monitor the course of the refinement procedure. Several cycles of rigid-body refinement in X-PLOR,[41] using force-field parameters derived by Engh and Huber,[42] were carried out and the resulting electron density map, viewed using the program O,[43] showed strong peaks in the $2F_o–F_c$ and $F_o–F_c$ maps for two zinc and two calcium atoms together with electron density in the active site for the inhibitor. Positive and negative density in the $F_o–F_c$ map indicated differences in amino acid sequence between SCD and GaCD. The correct sequence for GaCD was modelled into the $2|F_o| – |F_c|$ density. A glycine residue (190A) was inserted after residue 190 and residues 224–226 were removed as density in these regions (corresponding to VR1 and VR2) were both poor. Rigid-body refinement followed by conventional positional and then temperature factor refinement with a bulk-solvent correction gave $R_{free} = 0.336$ and $R = 0.278$. This gave excellent density for the third calcium and allowed the inhibitor to be unambiguously positioned in the GaCD active site. Residues at the N- and C-termini were defined by good electron density and added to the model. Further rounds of refinement and modelling allowed the variable regions, VR1 and VR2, at either side of the active site to be defined, although there was still very poor density for Lys190. Water molecules coordinating two of the calciums and the inhibitor were added to the model. The R_{free} and conventional R factor converged at 0.244 and 0.205 respectively.

RESULTS AND DISCUSSION

Overall Three-dimensional Structure

Figure 1 shows the structure of the catalytic domain of gelatinase A (GaCD), defined in this study, compared to that of stromelysin catalytic domain (SCD).[26,27] GaCD adopts the now familiar open-sandwich topology of matrix metalloproteinases, in which two α-helices are packed against a twisted, five-stranded β-sheet. The amphipathic helix α_A extends the full length of the sheet and is inserted between parallel β_1 and β_2. The strands are ordered $\beta_2\beta_1\beta_3\beta_5\beta_4$ in the sheet, with strand β_4 antiparallel to the others. Helix α_B contains the sequence HExxH, with the two histidines (201 and 205, stromelysin numbering, see Figure 2) positioned to be ligands to the catalytic zinc. A short turn at the conserved Gly208 brings His211 into a position in which it can be a third ligand for the catalytic zinc. The remaining part of the structure comprises turns and short strands together with helix α_C; these contribute to the formation of a well-defined substrate binding cleft.

Comparison of GaCD with the SCD Complexes

A comparison of the sequences and structural features of GaCD and other members of the matrixin family is shown in the JOY format[48,49] generated using the program COMPARER[50] (Figure 2). GaCD is most similar

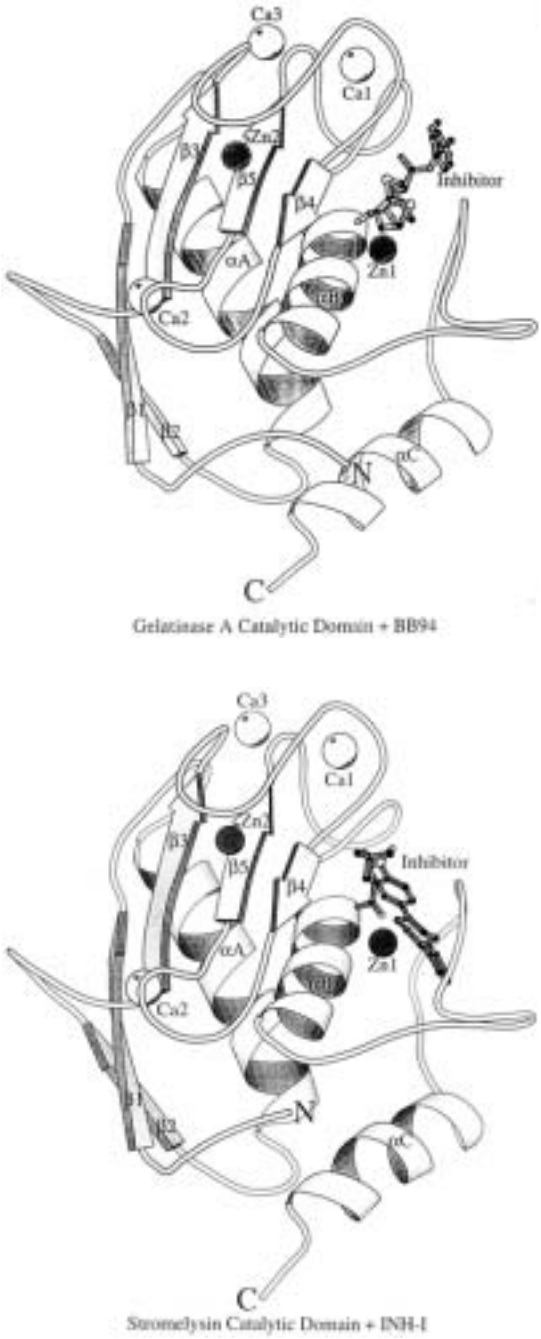

Figure 1. MOLSCRIPT[44] representation of the structure of (a) GaCD complexed with BB94 and (b) SCD complexed with INH-I.

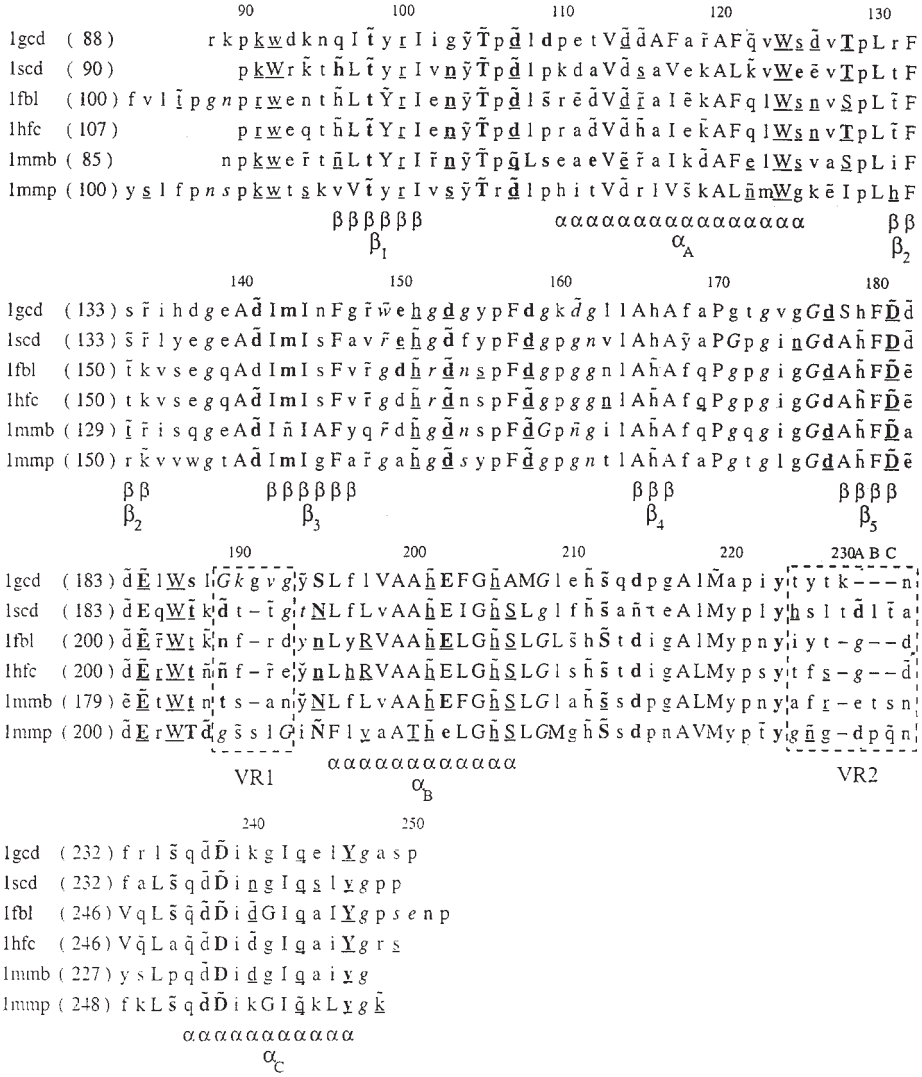

Figure 2. JOY format output[45] of the structural alignment of matrix metalloproteinases generated using COMPARER.[46] The variable regions VR1 (189–193) and VR2 (224–231) are bounded by dashed lines. The numbering is relative to that used for stromelysin. Protein codes are as follows: SCD, stromelysin catalytic domain complex with U24522; GaCD, Gelatinase A catalytic domain; 1FBL, full-length porcine synovial collagenase; 1HFC, human fibroblast collagenase catalytic domain; 1MMB, human neutrophil collagenase catalytic domain; 1MMP, human matrilysin. The alignment key is as follows: UPPER CASE, solvent inaccessible; lower case, solvent accessible; **bold type**, hydrogen bond to main-chain amide; underline, hydrogen bond to main-chain carbonyl; tilde, hydrogen bond to side-chain; *italics*, positive φ; çedilla, disulphide bonded cysteine; breve, *cis*-peptide.

to SCD followed by the collagenases and then by matrilysin. The core regions of GaCD show no significant difference to SCD. The main differences between GaCD and SCD occur at the site of the insertion in VR1 and at the three-residue deletion in VR2. Smaller differences are found in the region 135–140, which forms a loop between α_2 and α_3, and in the region 148–151, which forms a loop between α_3 and α_4; these adopt different conformations due to crystal packing. The N-terminus is more ordered than in SCD since it interacts with an equivalent region in a symmetry-related molecule (1+*x*, 1+*y*, *z*), with residue Asp141 (between strands α_2 and α_3), the loop containing residues 170–172 (between strands α_4 and α_5), and residue Leu245 in helix $\alpha_{C,}$ of the symmetry-related molecule.

Metal Coordination

The coordination of the catalytic Zn1 by His 201 Nε2, His205 Nε2 and His211 Ne2, described above, is completed by both hydroxamate oxygens of the inhibitor, in a distorted pentacoordinate geometry (Figure 3). A very similar environment is apparent in the SCD hydroxamate complex.[26,27] GaCD also coordinates the other two zincs and two calciums in a similar fashion to SCD. Thus, Zn2 is bound in a tetrahedral coordination by His151 Nε2, Asp153 Oδ2, His166 Nε2, and His179 Nδ1. All three calciums are octahedrally coordinated by six ligands. Ca1 is bound by Asp158 Od1, Gly159 O, Asp161 O (Gly161 in SCD), Leu163 O (Val163 in SCD), Asp181 Oδ2, and Glu184 Oε2, Ca2 by Asp141 O, Gly173 O, Gly175 O (Asn175 in SCD), Asp177 Oδ1 and waters, and Ca3 by Asp107 Oδ2, Asp182 Oδ1, Asp182 O, Glu184 O, and two waters.

Inhibitor Binding

The S1' specificity sites in SCD and GaCD are perhaps best described as tunnels and differ from the smaller pockets found in fibroblast collagenase and matrilysin. In SCD and GaCD they are roughly the same size but are significantly different in shape. This results partly from the three residue deletion 224–226 in GaCD relative to SCD. It also results from differences in specific residues; thus in GaCD, Thr227 points away from the S1' site rather than into it as found with His224 in SCD. Differences in residues 226–232 in GaCD also result in an additional bulge, and hence GaCD is more accommodating to inhibitors with large, 'kinked' groups, in contrast to the near-linear structure of most MMP inhibitors of SCD.[29,41] Differences in the conformation of residues 222–225, particularly Ile222 (Leu222 in SCD) lead to a much smaller S2' site in GaCD.

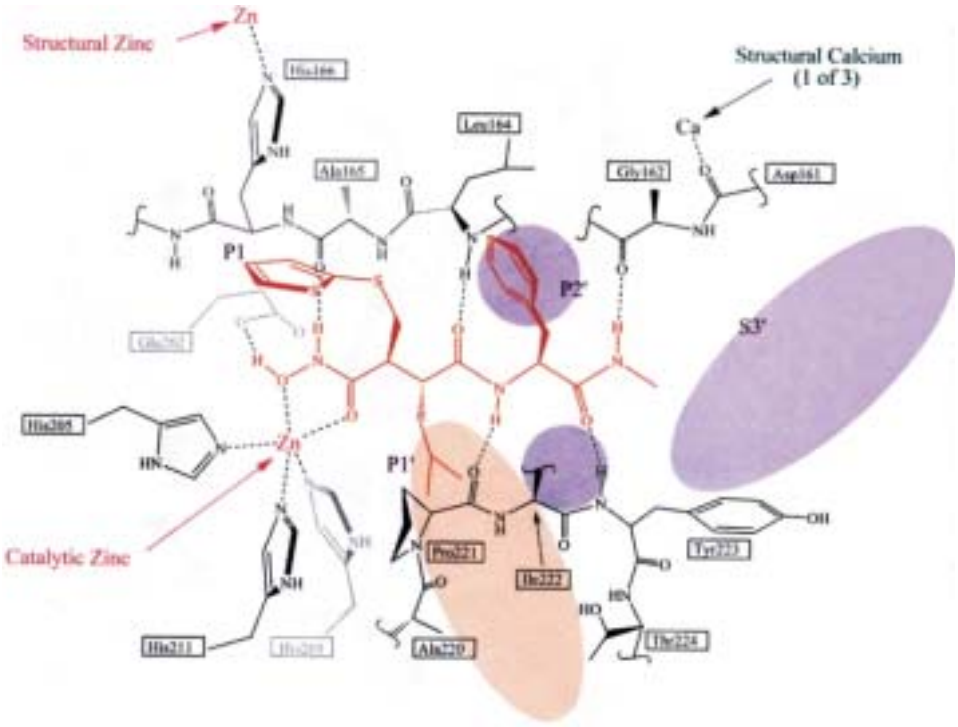

Figure 3. The binding of BB94 with GaCD.

BB94 is a dipeptidic hydroxamate inhibitor (see Figure 4) which spans the GaCD subsites S1' and S2'. The inhibitor forms a complementary strand to β_4 and binds the zinc, similar to other hydroxamate inhibitor complexes of MMPs. As in the U24522-SCD complex (see Figures 4 and 5a), five hydrogen bonds are formed between the inhibitor main chain and the protein (see Figure 5b). One of the chelating oxygens, O3, forms hydrogen bonds with three groups in close proximity, a water, Glu202 Oε1, and Ala165 O.

The P1' leucine of the inhibitor is surrounded by residues Leu164, Val198, Pro221, and Tyr223 (as in the SCD complex), which line the entrance to the deep S1' subsite. The P2' phenylalanine of the inhibitor forms contacts with Leu163 and Ile222 which line the shallow S2' subsite. As can be seen from Figure 2, these residues are different in SCD and the other matrixins.

In order to gauge the relative size and shape of the S1' site, inhibitor INH-I from its complex with SCD[38] (see Figure 4) was superimposed onto

BB94

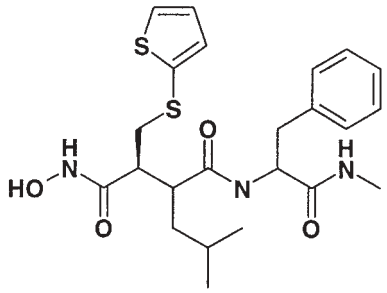

INH-I

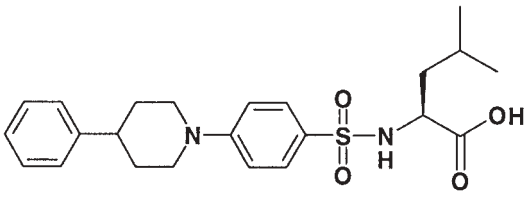

U24522

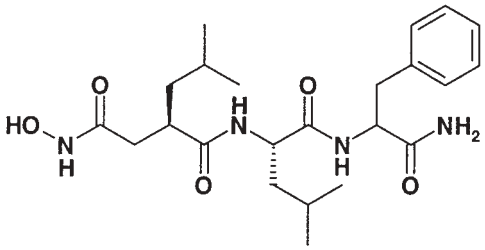

Figure 4. Schematic drawings of the inhibitors: BB94, INH-I, and U24522.

Figure 5. LIGPLOT [47] of the active site of: (a) SCD complexed with U24522; (b) GaCD complexed with BB94; (c) INH-I superimposed on GaCD. The program HBPLUS[48] was used to calculate hydrogen bonds and hydrophobic contacts between ligand and protein using the default criteria. The hydrophobic contacts are represented as spokes protruding from a ligand atom to a protein atom or residue (denoted as an arc). Spokes radiating toward the ligand indicate a potential interaction. The zinc ions and water molecules and their subsequent bonding interactions are not shown. ⇒

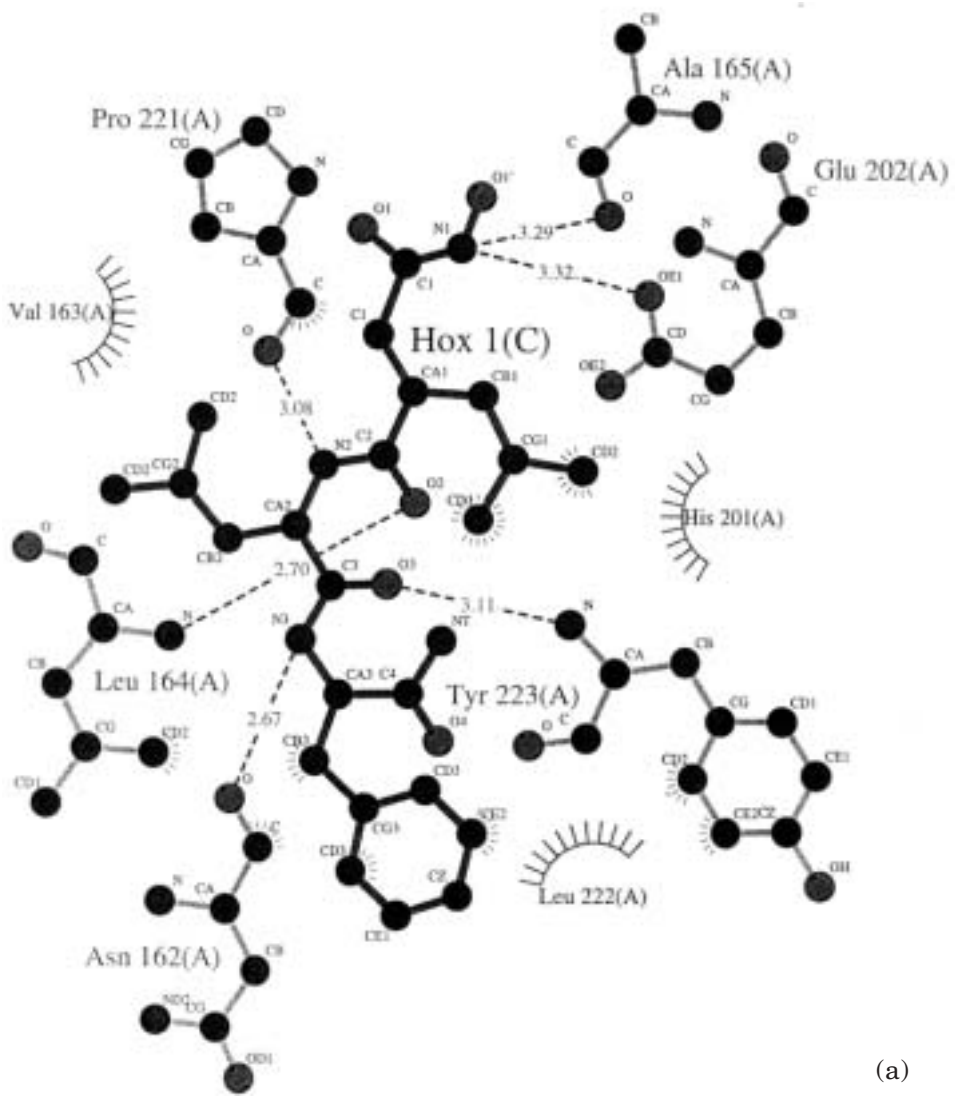

(a)

Key

- Ligand bond
- Non-ligand bond
- Hydrogen bond and its length
- His 33 Non-ligand residues involved in hydrophobic contact(s)
- Corresponding atoms involved in hydrophobic contact(s)

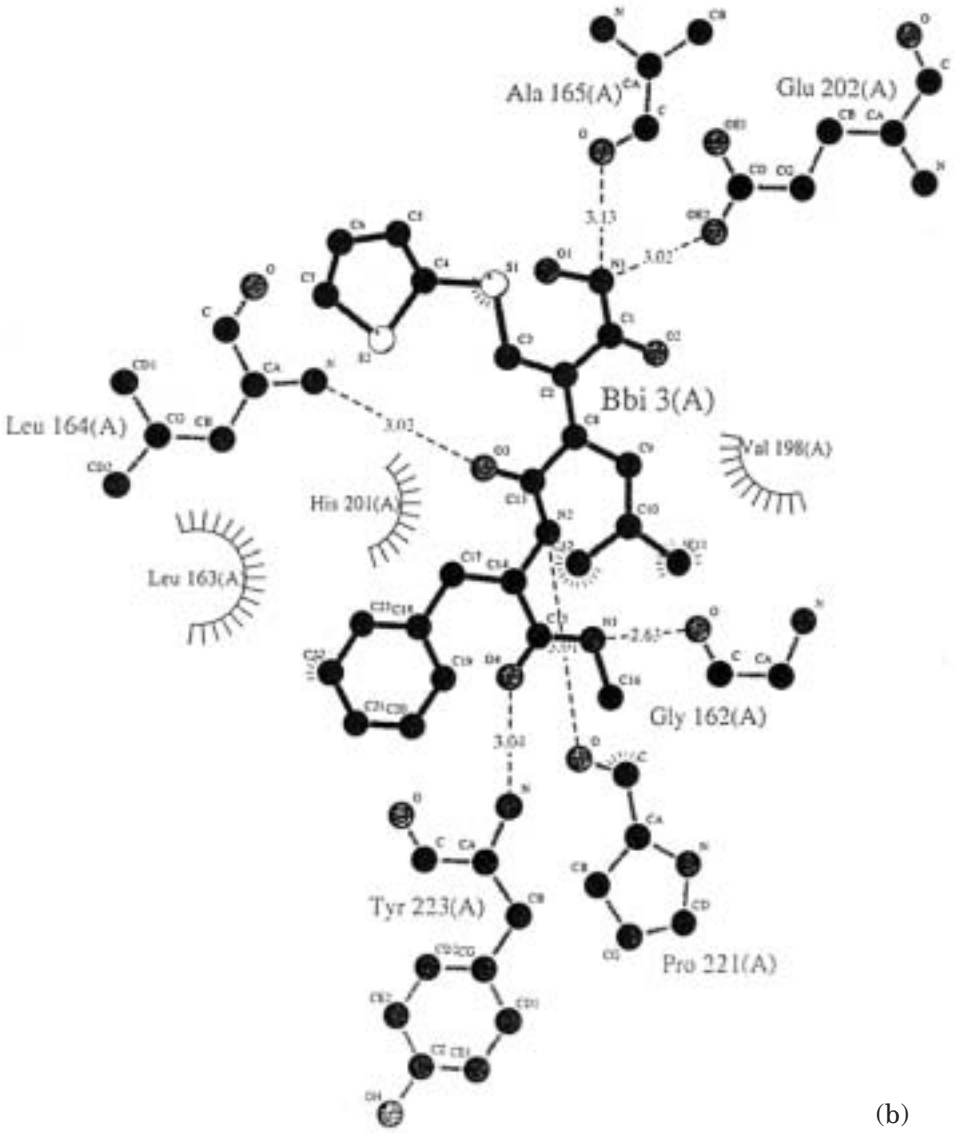

(b)

Key

Ligand bond

Non-ligand bond

Hydrogen bond and its length

His 53 Non-ligand residues involved in hydrophobic contact(s)

Corresponding atoms involved in hydrophobic contact(s)

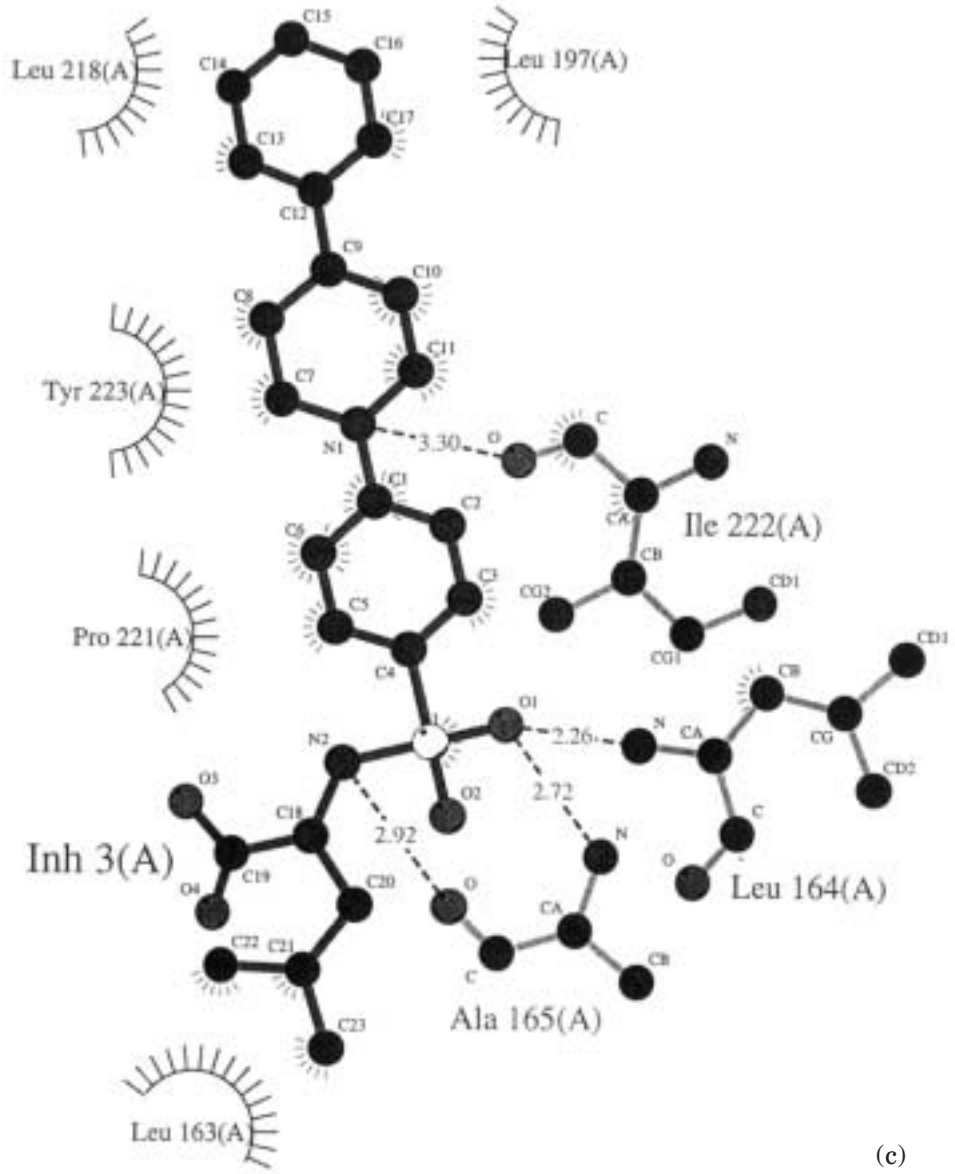

(c)

Key

Ligand bond

Non-ligand bond

Hydrogen bond and its length

His 53 Non-ligand residues involved in hydrophobic contact(s)

Corresponding atoms involved in hydrophobic contact(s)

the active site of GaCD (see Figure 5c). The inhibitor maintains the hydrogen bonding of the corresponding SCD structure, and makes a new contact between N1 and Ile222 O. The inhibitor also makes good hydrophobic contacts in the S1' site with Pro221, Tyr223, Leu218, Leu197, and Ile222 (Leu222 in SCD) as in the SCD complex of INH-I,[38] along with Leu163 (Val163 in SCD) in the S2' site. However, there appears to be no / reduced contact with His201, Phe232, His224, and Leu226 (the last two being part of the 3-residue deletion in the sequence of GaCD relative to SCD).

GaCD and SCD appear to have larger S1' sites compared to the other matrix metalloproteinases for which crystal structures are available. In the fibroblast collagenases (1FBL and 1HFC), the S1' site is significantly smaller due to the fact that Arg214 (collagenase numbering) impinges on this area and would clash with the piperidine ring and the distal phenyl group of INH-I. A similar clash with Tyr214 would occur with the inhibitor in matrilysin (1MMP). In neutrophil collagenase (1MMB), Arg222 (collagenase numbering) would clash with the tip of the distal phenyl ring of the inhibitor, implying that its S1' site is deeper than in the fibroblast collagenases and matrilysin but smaller than in stromelysin and gelatinase.

Crystal Packing

In some SCD complexes[26,29,38] the D^{153}FYP residues are part of an exposed loop which binds into the non-prime substrate binding site of a neighbouring SCD molecule related by a non-crystallographic 2-fold axis. Interestingly the equivalent sequence in GaCD, D^{153}GYP, is also involved in intramolecular interactions.

The intermolecular packing leads to large solvent channels in the crystal lattice, one of which lies in the centre of the unit cell, parallel to the 4_1 axis along c. It is interesting to note that the active site of GaCD, including some of the inhibitor side chains, lead directly into this channel.

Acknowledgements. – We thank colleagues at SRS, Daresbury for the allocation of beamtime which was used to collect intensity data.

Note added in proof. – The structure of human pro-matrix metalloproteinase-2 has now been published (E. Morgunova *et al.*, 1999).[49]

REFERENCES

1. J. F. Woessner, *FASEB J.* **5** (1991) 2145–2154.
2. R. P. Beckett, A. H. Davidson, A. H. Drummond, P. Huxley, and M. Whittaker, *Drug Discovery Today* **1** (1996) 16–26.
3. B. Davies, P. D. Brown, N. East, M. J. Crimmin, and F. R. Balkwill, *Cancer Res.* **53** (1993) 2087–2091.
4. X. Wang, X. Fu, P. D. Brown, M. J. Crimmin, and R. M. Hoffman, *Cancer Res.* **54** (1994) 4726–4728.
5. P. D. Brown, *Ann. N. Y. Acad. Sci.* **732** (1994) 217–221.
6. W. Bode, F-X. Gomis-Rüth, and W. Stöcker, *FEBS Lett.* **331** (1993) 134–140.
7. A. I. Marcy, L. L. Eiberger, R. Harrison, H. K. Chan, N. I. Hutchinson, W. K. Hagmann, P. M. Cameron, D. A. Boulton, and J. D. Hermes, *Biochemistry* **30** (1991) 6476–6483.
8. C. L. Lowry, G. McGeehan, and H. LeVine, *Proteins* **12** (1992) 42–48.
9. R.Sanchez-Lopez, C.M. Alexander, O.Behrendtsen, R. Breathnach and Z.Werb, *J. Biol. Chem.* **268** (1993) 7238–7247.
10. S. Schnierer, T. Kleine, T. Gote, A. Hillemann, V. Knäuper, and H. Tschesche, *Biochem. Biophys. Res. Commun.* **191** (1993) 319–326.
11. Q. Z. Ye, L. L. Johnson, I. Nordan, D. Hupe, and L. Hupe, *J. Med. Chem.* **37** (1994) 206–209.
12. N. Borkakoti, F. K.Winkler, D. H. Williams, A. D'Arcy, M. J. Broadhurst, P. A. Brown, W. H. Johnson. and E. J. Murray, *Nature (London) Struct. Biol.* **1** (1994) 106–110.
13. B. Lovejoy, A. Cleasby, A. M. Hassell, K. Longley, M. A. Luther, D. Weigl, G. Mc Geehan, A. B. McElroy, D. Drewry, M. H. Lambert, and S. R. Jordan, *Science* **263** (1994) 375–377.
14. B. Lovejoy, A. M. Hassell, M. A. Luther, D. Weigl, and S. R. Jordan, *Biochemistry* **33** (1994) 8207–8217.
15. J. C. Spurlino, A. M. Smallwood, D. D. Carlton, T. M. Banks, K. J. Vavra, J. S. Johnson, E. R. Cook, J. Falvo, R. C. Wahl, T. A. Pulvino, J. J. Wendolski and D. L. Smith, *Proteins* **19** (1994) 98–109.
16. W. Bode, P. Reinemer, R. Huber, T. Kleine, S. Schnierer, and H. Tschesche, *EMBO J.* **13** (1994) 1263–1269.
17. P. Reinemer, F. Grams, R. Huber, T. Kleine, S. Schnierer, M. Pieper, H. Tschesche, and W. Bode, *FEBS Lett.* **338** (1994) 227–233.
18. T. Stams, J. C. Spurlino, D. L. Smith, R. C. Wahl, T. F. Ho, M. W. Qorronfleh, T. M. Banks, and B. Rubin, *Nature (London) Struct. Biol.* **1** (1994) 119–123.
19. F. Grams, P. Reinemer, J. C. Powers, T. Kleine, M. Pieper, H. Tschesche, R. Huber, and W. Bode, *Eur. J. Biochem.* **228** (1995) 830–841.
20. M. Betz, P. Huxley, S. J. Davies, Y. Mushtaq, M. Pieper, H. Tschesche, W. Bode, and F. X. Gomis–Ruth, *Eur. J. Biochem.* **247** (1997) 356–363.
21. H. Brandstetter, R. A. Engh, E. G. von Roedern, L. Moroder, R. Huber, W. Bode, and F. Grams, *Protein Sci.* **7** (1998) 1303–1309.
22. M. F. Browner, W. W. Smith, and A. L. Castelhano, *Biochemistry* **34** (1995) 6602–6610.
23. P. R. Gooley, J. F. O'Connell, A. I. Marcy, G. C. Cuca, S. P. Salowe, B. L. Bush, J. D. Hermes, C. K. Esser, W. K. Hagmann, J. P. Springer, and B. A. Johnson, *Nature (London) Struct. Biol.* **1** (1994) 111–118.

24. J. W. Becker, A. I. Marcy, L. L. Rokosz, M. G. Axel, J. J. Burbaum, P. M. D. Fitzgerald, P. M. Cameron, C. K. Esser, W. K. Hagmann, J. D. Hermes, and J. P. Springer, *Protein Sci.* **4** (1995) 1966–1976.
25. S. R. Van Doren, A. V. Kurochkin, W. Hu, Q-Z. Ye, L. L. Johnson, D. J. Hupe, and E. R. P. Zuiderweg, *Protein Sci.* **4** (1995) 2487–2498.
26. V. Dhanaraj, Q-Z. Ye, L. L. Johnson, D. J. Hupe, D. F. Ortwine, J. B. Dunbar, Jr., J. R. Rubin, A. Pavlovsky, C. Humblet, and T. L. Blundell, *Structure* **4** (1996) 375–386.
27. V. Dhanaraj, Q-Z. Ye, L. L. Johnson, D. J. Hupe, D. F. Ortwine, J. B. Dunbar, Jr., J. R. Rubin, A. Pavlovsky, C. Humblet and T. L. Blundell, *Drug Design and Discovery* **13** (1996) 3–14.
28. F-X. Gomis-Rüth, K. Maskos, M. Betz, A. Bergner, R. Huber, K. Suzuki, N. Yoshida, H. Nagase, K. Brew, G. P. Bourenkov, H. Bartunik, and W. Bode, *Nature* **389** (1997) 77–80.
29. A. G. Pavlovsky, M. G. Williams, Q-Z. Ye, D. F. Ortwine, C. F. Purchase III, A. D. White, V. Dhanaraj, B. D. Roth, L. L. Johnson, D. Hupe, C. Humblet, and T. L. Blundell, *Protein Sci*. (1999) accepted for publication.
30. C. Fernandez-Catalan, W. Bode, R. Huber, D. Turk, J. J. Calvete, A. Lichte, H. Tschesche and K. Maskos, *EMBO J.* **17** (1998) 5238–5248.
31. J. Li, P. Brick, M. C. O'Hare, T. Skarzynski, L. F. Lloyd, V. A. Curry, I. M. Clark, H. F. Bigg, B. L. Hazleman, T. E. Cawston, and D. M. Blow, *Structure* **3** (1995) 541–549.
32. Q.-Z. Ye, D. Hupe, and L. L. Johnson, *Curr. Med. Chem.* **3** (1996) 407–418.
33. Q.-Z.Ye, L. L. Johnson, A. E. Yu, and D. Hupe, *Biochemistry* **34** (1995) 4702–4708.
34. I. Massova, R. Fridman, and S. Mobashery, *J. Mol. Model.* **3** (1997) 17–30.
35. D. F.Ortwine, V. Dhanaraj, J. B. Dunbar, Jr., L. L. Johnson, A. G. Pavlovsky, C. F. Purchase III, A. D. White, M. G. Williams, and Q.-Z. Ye, 214th. ACS National Meeting, Las Vegas, NV, COMP 186. September 1997.
36. Z. Otwinowski and W. Minor, *Methods Enz.* **276** (1997) 307–326.
37. J. Navaza, *Acta Crystallogr., Sect. A* **50** (1994) 157–163.
38. M. G. Williams, Q.-Z. Ye, F. Molina, L. L. Johnson, D. F. Ortwine, A. Pavlovsky, J. R. Rubin, R. W. Skeean, A. D. White, T. L. Blundell, C. Humblet, D. J. Hupe, and V. Dhanaraj (1999), unpublished work.
39. G. J. Kleywegt and T. A. Jones, *Acta Crystallogr., Sect. D* **52** (1996) 826–828.
40. A. T. Brünger, *Nature* **355** (1992) 472–474.
41. A. T. Brünger, *X-PLOR: A System for X-ray Crystallography and NMR,* Yale University Press, New Haven, CT., 1993.
42. R. A. Engh and R. Huber, *Acta Crystallogr., Sect. A* **47** (1991) 392–400.
43. T. A. Jones, J-Y. Zou, S. W. Cowan, and M. Kjeldgaard, *Acta Crystallogr., Sect. A* **47** (1991) 110–119.
44. P. J. Kraulis, *J. Appl. Crystallogr.* **24** (1991) 946–950.
45. J. P. Overington, M. S. Johnson, A. Šali, and T. L. Blundell, *Proc. R. Soc. London Biol.* **241** (1990) 132–145.
46. A. Šali and T. L. Blundell, *J. Mol. Biol.* **212** (1990) 403–428.
47. A. C. Wallace, R. A. Laskowski and J. M. Thornton, *Protein Eng.* **8** (1995) 127–134.
48. I. K. McDonald and J. M. Thornton, *J. Mol. Biol.* **238** (1994) 777–793.
49. Reference for *Note* added in proof:
E. Morgunova, A. Tuuttila, U. Bergman, M. Isupov, Y. Lindquist, G. Schneider, and K. Tryggvason, *Science* **284** (1999) 1667–1670.

SAŽETAK

Rentgenska struktura katalitičkog područja gelatinaze A kompleksirane hidroksamatnim inhibitorom

Venugopal Dhanaraj, Mark G. Williams, Qi-Zhuang Ye, Franck Molina, Linda L. Johnson, Daniel F. Ortwine, Alexander Pavlovsky, J. Ron Rubin, Richard W. Skeean, Andy D. White, Christine Humblet, Donald J. Hupe i Tom L. Blundell

Gelatinaza A ključni je enzim u skupini matričnih metaloproteinaza (matriksina) koje su uključene u degradaciju izvanstanične matrice. Kako je taj proces sastavni dio metastaze i angiogeneze tumorne stanice, gelatinaza je važna meta pri terapiji. Rentgenska kristalna struktura katalitičkog područja gelatinaze A (GaCD) kompleksiranog hidroksamatnim inhibitorom, batimastatom (BB94), pokazuje aktivno mjesto s velikim S1' specifičnim džepom. Struktura je slična prethodno riješenim strukturama katalitičkog područja stromelizina (SCD), ali s razlikama u VR1 i VR2, dvama površinski izloženim petljama na svakoj strani prolaza prema aktivnom mjestu. Usporedba GaCD s drugim članovima skupine matričnih metaloproteinaza ističe očuvanje ključnih sekundarnih strukturnih elemenata i značajnu razliku u specifičnom džepu, a to su ona znanja koja će povećati mogućnosti oblikovanja svojstvenih inhibitora za tu važnu antitumornu metu.